



## ORIGINAL ARTICLE

# Selective removal of Cd(II), As(III), Pb(II) and Cr(III) ions from water resources using novel 2-anthracene ammonium-based magnetic ionic liquids



Ahmed Abdi Hassan<sup>a</sup>, Abdulkadir Tanimu<sup>b</sup>, Saheed A. Ganiyu<sup>a,b</sup>,  
Ibrahim Y. Yaagoob<sup>a</sup>, Khalid Alhooshani<sup>a,b,\*</sup>

<sup>a</sup> Department of Chemistry, King Fahd University of Petroleum and Minerals, Dhahran 31261, Saudi Arabia

<sup>b</sup> Center for Refining and Advanced Chemicals, Research Institute, King Fahd University of Petroleum and Minerals, Dhahran 31261, Saudi Arabia

Received 16 April 2022; accepted 15 July 2022

Available online 20 July 2022

## KEYWORDS

2-anthracene;  
Magnetic ionic liquid;  
Adsorbent;  
Heavy metals;  
Wastewater;  
Adsorption capacity

**Abstract** Facile synthesis of two 2-anthracene ammonium-based magnetic ionic liquids (MILs), 2-anthracene ammonium tetrachloroferrate (III) ([2A-A]FeCl<sub>4</sub>) and 2-anthracene ammonium trichlorocobaltate (II) ([2A-A]CoCl<sub>3</sub>) was performed by protonation of 2-aminoanthracene, followed by complexation with FeCl<sub>3</sub>/CoCl<sub>2</sub>. The MILs were tested in the adsorptive removal of Cd<sup>2+</sup>, As<sup>3+</sup>, Pb<sup>2+</sup> and Cr<sup>3+</sup> from water sources. Upon treatment with 10 mg dosage of MILs in 10 mL aqueous solution of 50 ppm each of Cd<sup>2+</sup>, As<sup>3+</sup>, Pb<sup>2+</sup> and Cr<sup>3+</sup>, adsorption capacity (mg/g) in the range of 5.73–55.5 and 23.6–56.8 for [2A-A]FeCl<sub>4</sub> and [2A-A]CoCl<sub>3</sub> respectively were recorded. Thus, the optimization, kinetic and isotherms studies were conducted using the [2A-A]CoCl<sub>3</sub> adsorbent. The [2A-A]CoCl<sub>3</sub> was more effective in pH 7–9, and equilibrium adsorption was achieved after 60 min contact time. The adsorption process proceeded via the Pseudo-second order pathway and the Langmuir isotherm model is the best fit for the adsorption process (with  $q_{\max} = 227 - 357$  mg/g) of all the targeted metal ions. The [2A-A]CoCl<sub>3</sub> adsorbent demonstrated practicality with large distribution and selectivity coefficients of the targeted ions, and up to six times regeneration.

© 2022 The Author(s). Published by Elsevier B.V. on behalf of King Saud University. This is an open access article under the CC BY-NC-ND license (<http://creativecommons.org/licenses/by-nc-nd/4.0/>).

\* Corresponding author.

E-mail address: [hooshani@kfupm.edu.sa](mailto:hooshani@kfupm.edu.sa) (K. Alhooshani).

Peer review under responsibility of King Saud University.



## 1. Introduction

Water is essential to life, whether for humans, animals, or plants. Yet most people in the world today lack clean and safe drinking water. In addition, the world population is growing exponentially and in turn anthropogenic activities are increasing (Pendergast and Hoek, 2011). Moreover, urbanization and industrialization have significantly increased the demand for water and increased the pollution of all available sources. Therefore, there is an urgent need for effective treatment and reuse of wastewater, groundwater, surface water and runoff from agricultural activities (Hu et al., 2020; Tanimu et al., 2021). Undoubtedly, more than 70% of the problems in most developing countries are due to water pollution and contamination (Vardhan et al., 2019). Such contaminants are dyes (Hassan et al., 2020; Katheresan et al., 2018), heavy metals (Bolisetty et al., 2019; Vardhan et al., 2019), pesticides (Abdi Hassan et al., 2020; de Souza et al., 2020), pharmaceutical and drug related pollutants (Guo et al., 2017).

Heavy metals are metals or metalloids that have an atomic density greater than 4000 kg/m<sup>3</sup> (Hawkes, 1997). They are generally toxic even at trace concentrations, good examples are mercury, lead, cadmium, arsenic, and chromium (Pratush et al., 2018; Tanimu and Alhooshani, 2021). The adverse health effects of lead are particularly well documented in children, as their bodies can absorb 50% more of it than an adult's 10%. Accordingly, it has more dangerous consequences in children such as brain damage, kidney failure, learning problems, hearing and vision problems, complications of the cardiovascular system, liver and reproductive organs, and growth retardation. Moreover, in adults, especially in women, it causes reproductive problems and pregnancy complications in addition to memory loss and birth defects, etc., and in men, kidney failure, brain, and digestive damages are the main problem (Dinake et al., 2019). Chromium has different oxidation states ranging from -1 to + 6, but the most stable is + 3 and + 6. Cr (III) is associated with the absorption of glucose in the blood and causes an energy crisis in the body and is highly toxic, especially Cr (IV) is even more toxic than Cr (III). Largely, chromium is associated with carcinogenicity in humans and animals. It causes stomach and intestinal ulcers, respiratory problems, kidney problems, and liver damage, and affects the reproductive system in men (Almeida et al., 2019). Toxicity of Cr<sup>3+</sup> causes decrease in catalase and uricase enzymes activity and a gradual rise in the excretion of iron binding compound that are signs of conditional intracellular iron deficit causing anemia and more complex health problems (Ramana and Sastry, 1994). Cr<sup>3+</sup> is also non-biodegradable, mutagenic and genotoxic (Zhu et al., 2022).

Arsenic is the predominant inorganic contaminant in groundwater, especially As (III) which is more toxic and mobile than As (V). Arsenic forms complex, severe geochemical and biological reactions, making it difficult to deal with during removal and treatment (Korte and Fernando, 1991). Exposure to As leads to life-threatening health effects such as cancer, diabetes, cardiovascular problems, kidney problems, respiratory diseases, gastrointestinal complications, neurological and dermal effects and others (Maia et al., 2021). Besides, cadmium is a toxic metal ion and is also associated with carcinogenicity in humans and has severe health effects on organs such as kidney, liver, and lungs. Most of these heavy metals, including cadmium, originate from anthropogenic and human activities such as industry, mining, and burning of oil and coal. Moreover, the toxicity of Cd (II) is aggravated by its accumulation behavior (Pyrzynska, 2019; Erdem Yayayürük et al., 2021; Körpınar et al., 2021).

Therefore, proper removal of heavy metals from subsurface and wastewater is of utmost importance and various methods have been reported in the literature such as adsorption (Fiyadh et al., 2019), membrane separation (Khulbe and Matsuura, 2018), advanced oxidation (Azimi et al., 2017), ion exchange (Hassan and Carr, 2018), filtration (Hoslett et al., 2018), chemical oxidation (Yoo et al., 2017), biological methods (Ayangbenro and Babalola, 2017; Ojuederie and

Babalola, 2017), reverse osmosis (RO) (Joo and Tansel, 2015), etc. However, the most preferred of these methods is adsorption due to its low cost and simplicity of approach specifically in wastewater treatment and has a wider application in industrial wastewater for the removal of metal ions (Gokmen et al., 2021; Lakherwal, 2014). Although the selection of the right adsorbent is key to the adsorption process, activated carbon is still the best option because it is commercially available and has a very high porosity, but the high cost associated to it is a major drawback (Renge et al., 2012). Therefore, the development of low cost and effective adsorbents for the removal of heavy metals from wastewater, groundwater and industrial effluents is an interesting area of research for scientists. Ionic liquids and magnetized ionic liquids are potential adsorbents for metal ions due to their polarity and charged properties that can easily promote electrostatic interactions (Fuerhacker et al., 2012; Kakaei et al., 2020; Stojanovic and Keppler, 2012; Wieszczycka et al., 2020; Xu et al., 2021).

In this study, two new magnetic ionic liquids (MILs), 2-anthracene ammonium tetrachloroferrate (III) ([2-AA]FeCl<sub>4</sub>) and 2-anthracene ammonium trichlorocobaltate (II) ([2-AA]CoCl<sub>3</sub>), were synthesized and used as adsorbents at room temperature for the removal of various metal ions (Cd<sup>2+</sup>, As<sup>3+</sup>, Pb<sup>2+</sup>, and Cr<sup>3+</sup>) from raw groundwater and wastewater sources. However, polyaromatic hydrocarbons commonly known as PAHs are classified as organic pollutants, but their conversion into useful materials taking advantage of their low solubility in water and easy modification due to the availability of the lone pairs of the amino group makes them an interesting material and creates new research direction.

## 2. Experimental

### 2.1. Materials

All chemicals were used as received without further purification. Ethanol, hydrochloric acid, calcium chloride, potassium chloride, magnesium chloride, sodium chloride, cobalt (II) chloride hexahydrate, 2-aminoanthracene were received from Sigma-Aldrich, USA. Ferric chloride was purchased from Fluka Analytical, Cadmium nitrate tetrahydrate, arsenic trichloride, lead (ii) nitrate, and chromium (iii) nitrate nonahydrate (99%) were acquired from Merck Chemicals, USA.

### 2.2. Synthesis of 2-anthracene ammonium-based magnetic ionic liquids

The synthesis procedure involved two steps, as previously reported (Hassan et al., 2021, 2020). In the first step, 3 M HCl in ethanol solvent was added to 2-aminoanthracene ([2-AA]) in a round bottom flask and the solution was vigorously stirred for 4 h, to form anthracene-2-aminium chloride ([2-AA]Cl) as an intermediate. The ethanol solvent in the reaction flask was removed using rotary evaporator, then the [2-AA]Cl intermediate was washed with deionized water to about pH 3.5 to remove the excess acid. Thereafter, an equimolar amount of FeCl<sub>3</sub> or CoCl<sub>2</sub> in ethanol was added into the flask containing the [2-AA]Cl intermediate and stirred for 24 h to form 2-anthracene ammonium tetrachloroferrate (III) or 2-anthracene ammonium trichlorocobaltate (II) respectively. The final product was washed several times until there were no traces of Fe<sup>3+</sup> or Co<sup>2+</sup> in the supernatant liquid. The summary of the synthesis steps has been provided in Fig. 1.

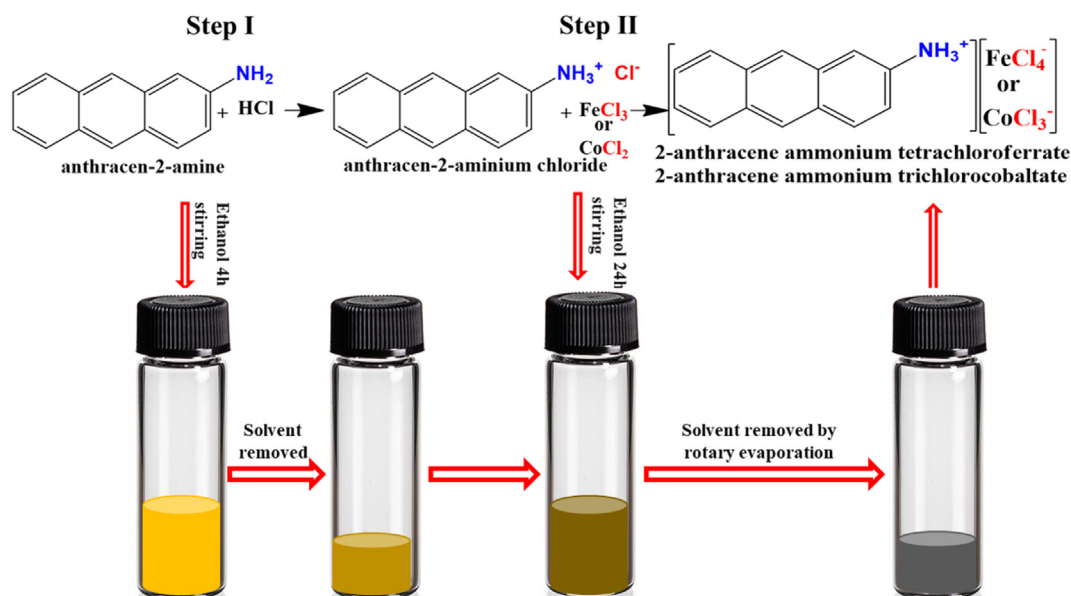


**Fig. 1** Synthesis procedure for 2-anthracene ammonium-based magnetic ionic liquids. The vials represent 2-anthracene ammonium tetrachloroferrate (III) formation.

### 2.3. Characterization of 2-anthracene ammonium-based magnetic ionic liquids

The <sup>1</sup>H NMR spectra of the starting material 2-AA and the intermediate [2-AA]Cl were recorded on the Bruker NMR 400 MHz model AVANCE 3. Fourier Transform Infrared (FTIR) spectra of the 2-AA, [2-AA]Cl intermediate and the ionic liquid adsorbents were recorded between 4000 cm<sup>-1</sup> and 400 cm<sup>-1</sup> using the Smart iTR NICOLET iS10 model. The thermogravimetric (TGA) analysis was carried out on a Thermogravimetric analyzer model SDT Q600 instrument. About 10 mg of the MIL was heated over a temperature range of 30 to 900 °C in an alumina pan at the rate of 10 °C/min with a nitrogen flow of 50 mL/min to obtain the decomposition curve. The UV/Vis absorption spectrum was measured on a UV/Vis spectrophotometer (Genesys 10S Thermo Fisher scientific, USA). The adsorbents were dissolved in ethanol to form about 1 × 10<sup>-3</sup> M concentration, then inserted into the sample cuvettes for spectrum measurement. Zeta potential of the MIL adsorbents was recorded using the model Analyzer Zeta PALS. Six different pH values in the range 2 – 12 were studied as a function of zeta potential (mV). DaynaCool (Quantum Design, US) instrument was used to measure the magnetization properties of the MILs. About 27.2 mg of each sample was loaded and both temperature and magnetic field varied. The morphology of [2-AA]CoCl<sub>3</sub> MIL before and after adsorption was studied using the Scanning Electron Microscopy (SEM) (JEOL JSM-6610LV instrument) and the constituent elements (in weight percent) were determined using Energy Dispersive X-Ray Analysis (EDX).

### 2.4. Heavy metals removal test

The heavy metals' adsorption experiment was carried out at room temperature in a batch system. A 10 mL aqueous solution containing the mixture of four heavy metal ions (Cd<sup>2+</sup>,

As<sup>3+</sup>, Pb<sup>2+</sup> and Cr<sup>3+</sup>) with initial concentrations ranging from 50 to 350 ppm was added to a 50 mL vial and adsorbent (5 – 30 mg) was subsequently dispersed into the heavy metal ions solution in the vial and sealed. The solution mixture was stirred for 5 min to 24 h until equilibrium is reached. Afterward, the adsorbent was isolated by centrifuging at 3500 rpm, and the supernatant was analyzed for heavy metal's presence using ICP-OES (PlasmaQuant® PQ 9000). The adsorption capacity ( $q_e$ , mg/g) of the heavy metal ions was determined using equation (1) below:

$$q_e = \left( \frac{V(C_i - C_e)}{m} \right) \quad (1)$$

Where V (L) represents the volume of the heavy metals' solution, C<sub>i</sub> and C<sub>e</sub> represent the initial and equilibrium concentrations of the solutions in mg/L. The m represents the mass of the adsorbents.

The effects of adsorption parameters such as pH, adsorbent dosage, contact time and concentration of heavy metal ions were studied following the same approach. The optimized adsorption conditions were extended to real wastewater and raw groundwater samples obtained from Khobar wastewater treatment plant and King Fahd University of Petroleum and Minerals (KFUPM) maintenance department respectively. The competitive adsorption of other metal ions (K<sup>+</sup>, Na<sup>+</sup>, Ca<sup>2+</sup> and Mg<sup>2+</sup>) and reusability studies of the adsorbents were performed.

## 3. Results and discussion

### 3.1. Characterization of 2-anthracene ammonium-based MIL adsorbents

#### 3.1.1. <sup>1</sup>H NMR spectra of 2-AA and [2-AA]Cl intermediate

The 2-AA spectrum (Fig. 2) shows the amine N-H protons at the chemical shift of 5.5 ppm. After protonation, the N-H sig-

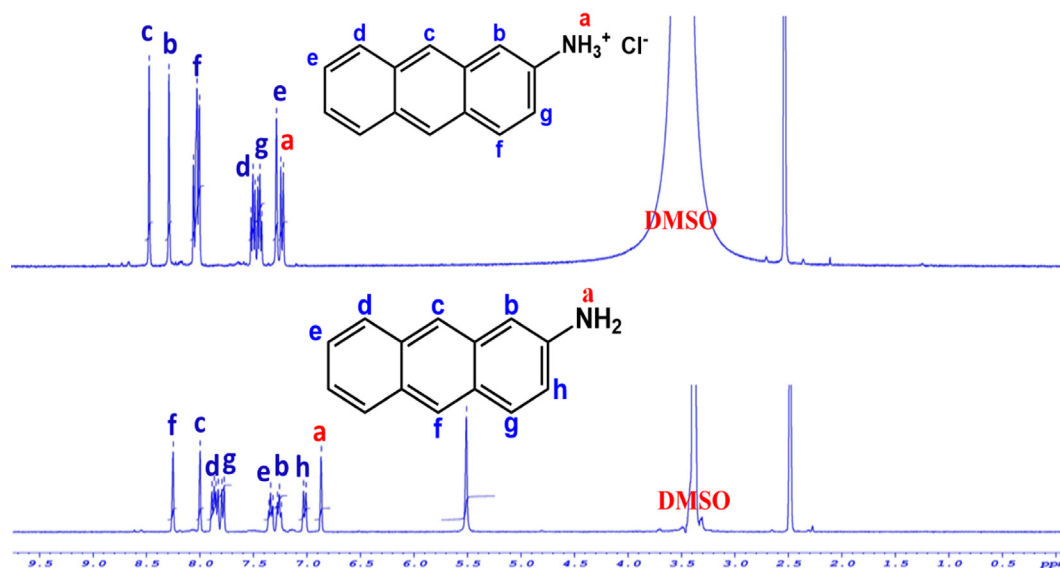


**Fig. 2**  $^1\text{H}$  NMR spectra of 2-aminoanthracene and anthracene ammonium chloride intermediate.

nal became very weak and was strongly shifted downfield to around  $\delta = 8\text{--}9$ . Similarly, all the C-H protons signals were downfield shifted by  $\delta = 0.3$ . Interesting, there were no additional peaks upon protonation of 2-AA to form [2-AA]Cl and the integral area peaks were directly proportional to the number of hydrogen atoms, which implies high purity of the [2-AA]Cl intermediate.

### 3.1.2. FTIR of [2-AA]CoCl<sub>3</sub> and [2-AA]FeCl<sub>4</sub> MIL adsorbents

The functional groups present in both 2-anthracene ammonium tetrachloroferrate (III) and 2-anthracene ammonium trichlorocobaltate (II) MIL adsorbents were elucidated using the FTIR. As presented in Fig. 3, the broad band observed between 3100 and 3400  $\text{cm}^{-1}$  are characteristics of stretching vibrations of the N-H bond in the adsorbents. Two peaks, one at 1590  $\text{cm}^{-1}$  owing to the  $\text{NH}_2$  scissoring mode and the other at 3300  $\text{cm}^{-1}$  due to the  $\nu(\text{N-H})$  stretching mode, are indicative of the amine group. Peaks observed below 1500  $\text{cm}^{-1}$  in the low-frequency portion of the spectra are caused by complex formation. The band seen at 2969.9  $\text{cm}^{-1}$  are C-H stretching vibrations due to the anthracene C-Hs. The skeletal vibrations of the rings are found at 1423.3  $\text{cm}^{-1}$  to 1650  $\text{cm}^{-1}$ , while the broad band at 3300 – 3500  $\text{cm}^{-1}$  in Fig. 3(c) and (d) is characteristic of OH stretching vibration due to the hygroscopic nature of the chlorides of cobalt and iron. The intermediate anthracene ammonium chloride's lack of sharp peaks at roughly 3300  $\text{cm}^{-1}$  is obviously caused by an acid-base complex formation of the  $\text{NH}_3^{3+}$ . The peak also observed at around 1615  $\text{cm}^{-1}$  to 1620  $\text{cm}^{-1}$  is caused by the  $\nu(\text{C} = \text{C})$  stretching mode and demonstrates that the  $\text{C} = \text{C}$  double bond is intact and not distorted. The characteristic behavior of the two MILs is considered similar and confirms the formation of the complex metal chlorides (Hassan et al., 2021; Yassin et al., 2015).

### 3.1.3. Thermogravimetric (TGA) analysis of [2-AA]CoCl<sub>3</sub> and [2-AA]FeCl<sub>4</sub> MIL adsorbents

The TGA decomposition curve of both MILs show similar decomposition pattern (Fig. 3(e)), with gradual decomposition

up to 400 °C for [2-AA]CoCl<sub>3</sub> and 500 °C for [2-AA]FeCl<sub>4</sub>. The decomposition below these temperatures is in three steps: first at 70 °C, which is ascribed to the melting point of the respective MILs, then at 150 °C, which is assigned to the loss of hydrated water molecules, and the sharp decrease observed above 300 °C is due to the decomposition of the respective MILs to form oxides. In general, the synthesized MILs have shown remarkable thermal stability with less than 10% weight loss up to 300 °C. This observation indicates that the magnetic moment to magnetic mass ratio is connected to the magnetization curves of the TGA. A similar observation was reported when cobalt was used in the synthesis of some MILs (Medeiros et al., 2012).

### 3.1.4. UV/Vis spectra of [2-AA]CoCl<sub>3</sub> and [2-AA]FeCl<sub>4</sub> MIL adsorbents

Superimposed UV–vis spectra of the starting material 2-aminoanthracene, the intermediate ion anthracene ammonium chloride, 2-anthracene ammonium tetrachloroferrate (III), and 2-anthracene ammonium trichlorocobaltate (II) was presented in Fig. 3(f). It was observed that all the spectra have similar pattern, however, the [2-AA]CoCl<sub>3</sub> and [2-AA]FeCl<sub>4</sub> MIL adsorbents show sharp and well resolved hypochromic shift peaks from 400 nm to 362 nm (indicated by the arrow). This can be associated with the stiffness introduced into the rings and confirms the formation of the corresponding complexes. Similar trend has been observed in previously reported MILs (Abdi Hassan et al., 2020; Yassin et al., 2015).

### 3.1.5. Zeta potential of [2-AA]CoCl<sub>3</sub> and [2-AA]FeCl<sub>4</sub> MIL adsorbents

The Zeta potential was measured as a function of pH dispersed in a double-distilled water, and the isoelectric point (IEP) was determined as the pH level at which the zeta potential is zero. The result of zeta potential measurement at different pH shown in Fig. 3(g) indicates that by increasing the pH above isoelectric point of 3.8 and 5.0, the interaction of the cationic moiety anthracene-2-aminium with the alkaline medium decreases, which is due to the repulsive forces generated by

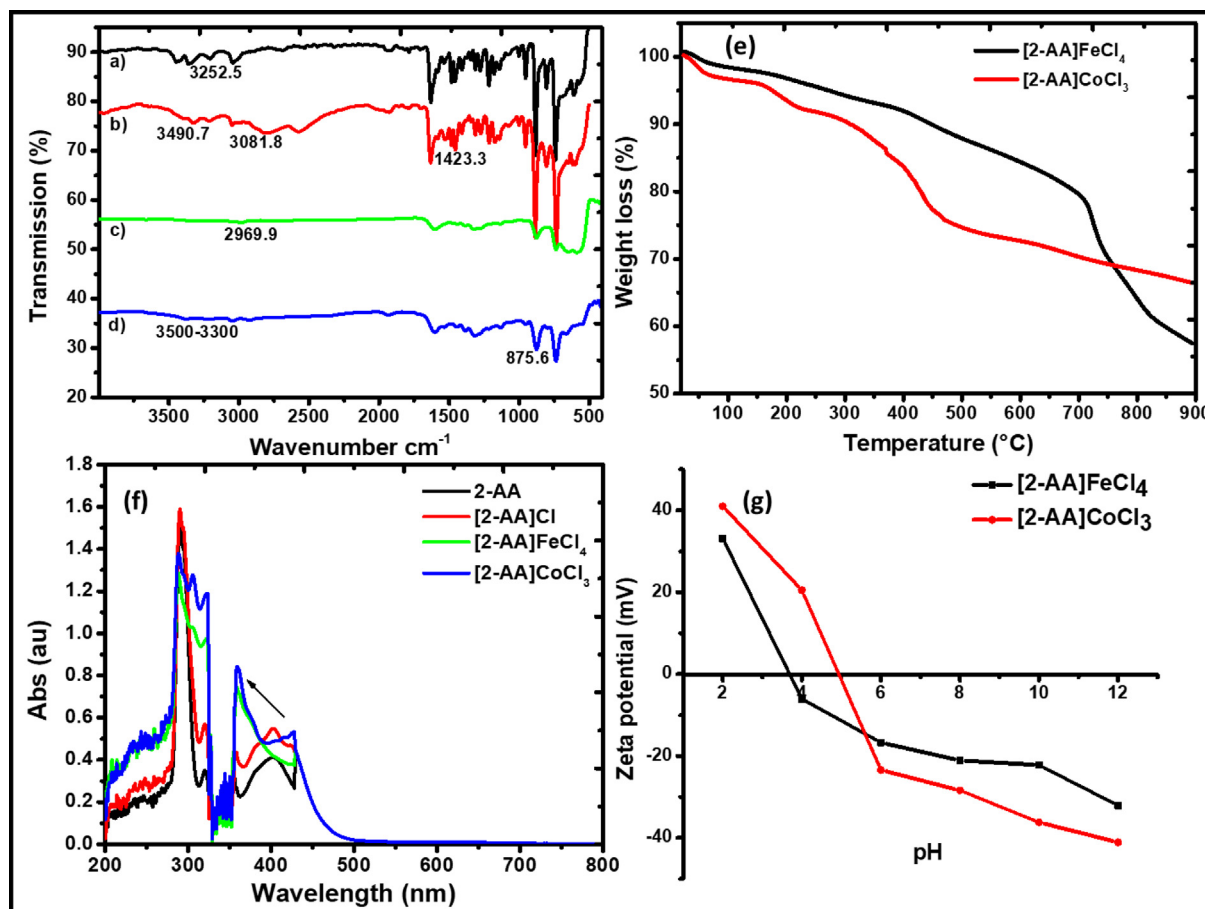


**Fig. 3** FTIR spectrum of: a) 2-aminoanthracene b) Intermediate anthracene ammonium chloride c) 2-anthracene ammonium tetrachloroferrate(III) d) 2-anthracene ammonium trichlorocobaltate(II); (e) TGA decomposition curve of [2-AA]FeCl<sub>4</sub> and [2-AA]CoCl<sub>3</sub>; (f) UV-vis spectra of 2-aminoanthracene, intermediate anthracene ammonium chloride, 2-anthracene ammonium tetrachloroferrate (III) and 2-anthracene ammonium trichlorocobaltate (II); (g) Zeta potential of MIL, 2-anthracene ammonium tetrachloroferrate (III) and 2-anthracene ammonium trichlorocobaltate (II).

the negative charges of the basic medium and FeCl<sub>4</sub> and similar behavior is observed in the two MILs. This indicates that the particles have both positive and negative charge. The higher mV values obtained are due to the presence of the aromatic rings (Breite et al., 2016; Sarkar et al., 2021).

### 3.1.6. Magnetization properties of [2-AA]CoCl<sub>3</sub> and [2-AA]FeCl<sub>4</sub> MIL adsorbents

The magnetization study indicates that [2-AA]FeCl<sub>4</sub> is ferromagnetic while is [2-AA]CoCl<sub>3</sub> superparamagnetic as shown by the s-shaped curve in Fig. 4(a) and Fig. 4(b). The superparamagnetic property of [2-AA]CoCl<sub>3</sub> is attributed to the crystal-lite size reduction, which decreases the anisotropy energy, hence favoring the superparamagnetism of the material. In addition, high saturation magnetization and high two-curie temperature of cobalt-containing MIL can be due to allotropic characteristics of the element. In the case of [2-AA]FeCl<sub>4</sub> which has depicted ferromagnetic property can be associated with the presence of iron which has a curie point at 770 °C and changes its crystalline structure above the curie point. It is also noted that in both samples, the temperature is directly proportional to the magnetic moment (Fig. 4(c) and Fig. 4

(d)), which agrees with Curie–Weiss law. Furthermore, a linear relationship between the magnetic field and the magnetization has been recorded and obtained at room temperature indicating that both MILs are magnetic. The magnetic susceptibility was found to be 1.17 and 1.16 for [2-AA]FeCl<sub>4</sub> and [2-AA]CoCl<sub>3</sub> respectively. This implies that both MILs have magnetic properties that can be attributed to iron and cobalt due to their structures which allow their electrons to line up more easily forming the magnetic field of the materials.

### 3.1.7. Morphological examination of [2-AA]CoCl<sub>3</sub> MIL adsorbent

The SEM image of [2-AA]CoCl<sub>3</sub> MIL before adsorption shows microparticle sizes with non-spherical, irregular shape, generally with fine texture, and non-uniform surface morphology (Fig. 5(a)). The thicker crystal-like structure observed after adsorption (Fig. 5(c)) is probably due to the presence of the adsorbed heavy metal ions on the surface of the [2-AA]CoCl<sub>3</sub> MIL adsorbent. In addition, the EDX spectrum shown in (Fig. 5(c)) confirms the presence of all the expected elements in their stoichiometric weight percentages in the [2-AA]CoCl<sub>3</sub> MIL adsorbent, while the EDX spectrum shown in (Fig. 5

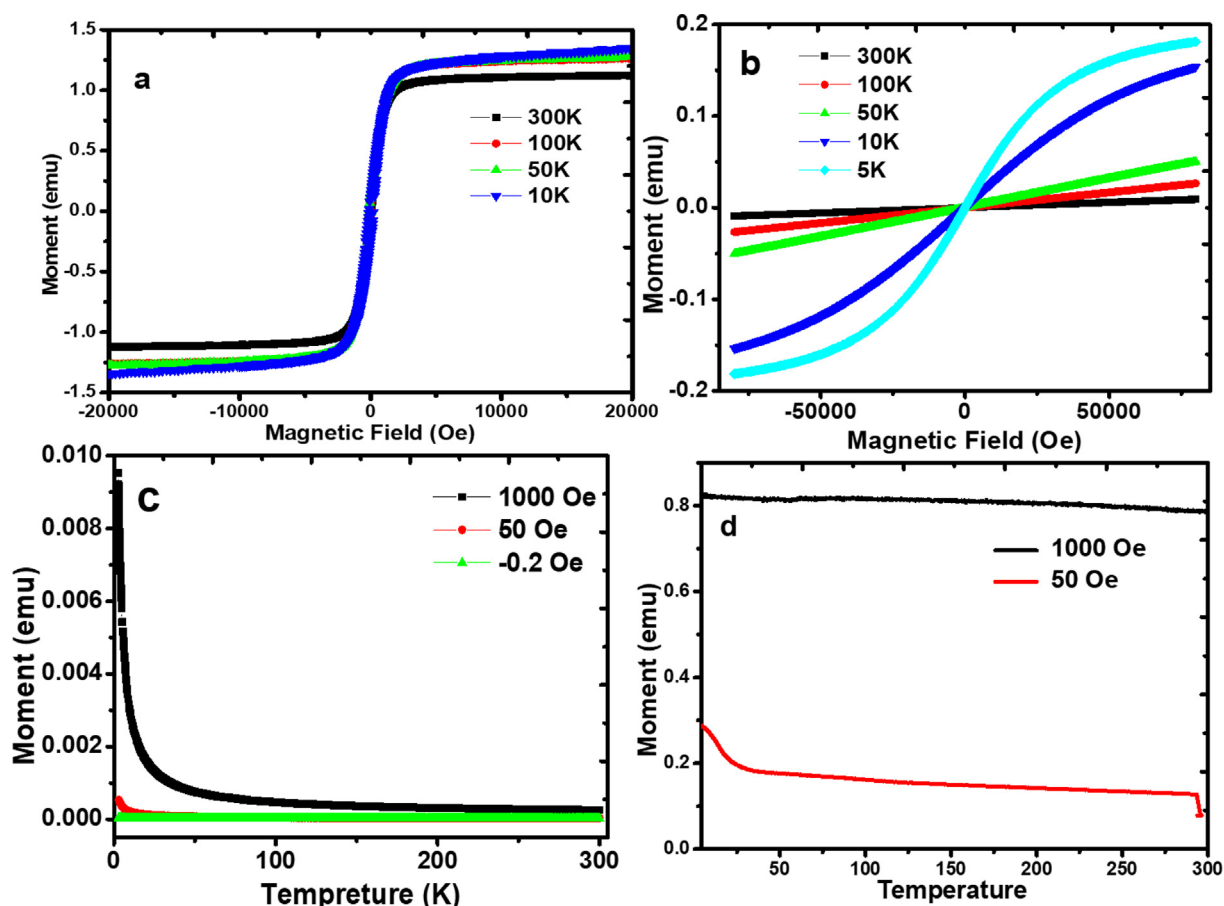


**Fig. 4** The magnetization of a) [2-AA]FeCl<sub>4</sub> as a function of the applied magnetic field at a temperature range of 10–300 K b) [2-AA]CoCl<sub>3</sub> as a function of the applied magnetic field at a temperature of 5–300 K c) [2-AA]CoCl<sub>3</sub> as a function of temperature in an applied magnetic field range of –0.2–1000 Oe and d) [2-AA]FeCl<sub>4</sub> as a function of temperature under an applied magnetic field of 50–1000 Oe.

(d) confirms the adsorption of the targeted heavy metal ions on the surface of [2-AA]CoCl<sub>3</sub> MIL adsorbent after the adsorption process.

### 3.2. Adsorption capacity of MIL adsorbents

The adsorption of heavy metal ions (Cd<sup>2+</sup>, As<sup>3+</sup>, Pb<sup>2+</sup> and Cr<sup>3+</sup>) was studied using 10 mg of either of [2-AA]CoCl<sub>3</sub> or [2-AA]FeCl<sub>4</sub> MIL adsorbents dispersed in 10 mL of metal ions containing solution (50 ppm each) and stirred for 24 h contact time. The obtained result, presented in Fig. 6(a), shows that both adsorbents have preferentially removed the targeted metal ions with adsorption capacity in the range of 5.73 – 55.5 mg/g for [2-AA]FeCl<sub>4</sub> and 23.6 – 56.8 mg/g for [2-AA]CoCl<sub>3</sub>. The stability against hydrolysis coming from carbon bond and cobalt bond in [2-AA]CoCl<sub>3</sub> is considered responsible for the relatively higher adsorption performance of the [2-AA]CoCl<sub>3</sub> when compared to the [2-AA]FeCl<sub>4</sub> counterpart and this can be attributed to d(z<sub>2</sub>) orbital which is occupied. Overall, both adsorbents have shown higher selectivity towards As<sup>3+</sup>, Pb<sup>2+</sup> and Cr<sup>3+</sup> with stronger binding sites compared to Cd<sup>2+</sup>. However, based on the obtained results, the [2-AA]CoCl<sub>3</sub> was adopted as the best adsorbent for the

removal of these heavy metal ions, and its adsorption parameters were subsequently optimized.

#### 3.2.1. Effect of [2-AA]CoCl<sub>3</sub> dosage on its adsorption capacity

The effect of [2-AA]CoCl<sub>3</sub> dosage on its adsorption capacity for removal of Cd<sup>2+</sup>, As<sup>3+</sup>, Pb<sup>2+</sup> and Cr<sup>3+</sup> was studied by varying the adsorbent dosage from 3 to 30 mg. The adsorption experiment was carried out by dispersing the adsorbent in 10 mL solution of 100 ppm each of metal ions, then stirred for 24 h contact time. It was observed that the percent removal of the heavy metals increases with increase in the dosage up to 30 mg. However, the adsorption capacity (which factors in the mass of adsorbent, as shown in equation (1)) increases from 3 to 5 mg, then decreases up to 30 mg (Fig. 6b). Therefore, the optimized adsorbent dosage is 5 mg.

#### 3.2.2. Effect of solution pH on the adsorption efficiency of [2-AA]CoCl<sub>3</sub>

The pH plays a significant role in the adsorption capacity, as it can affect both the metal speciation through the hydrolysis reaction and the electrostatic interaction between the adsorbent and the adsorbate (Wang et al., 2013). In this regard, a wide pH range (2 – 9) was investigated in the adsorption exper-

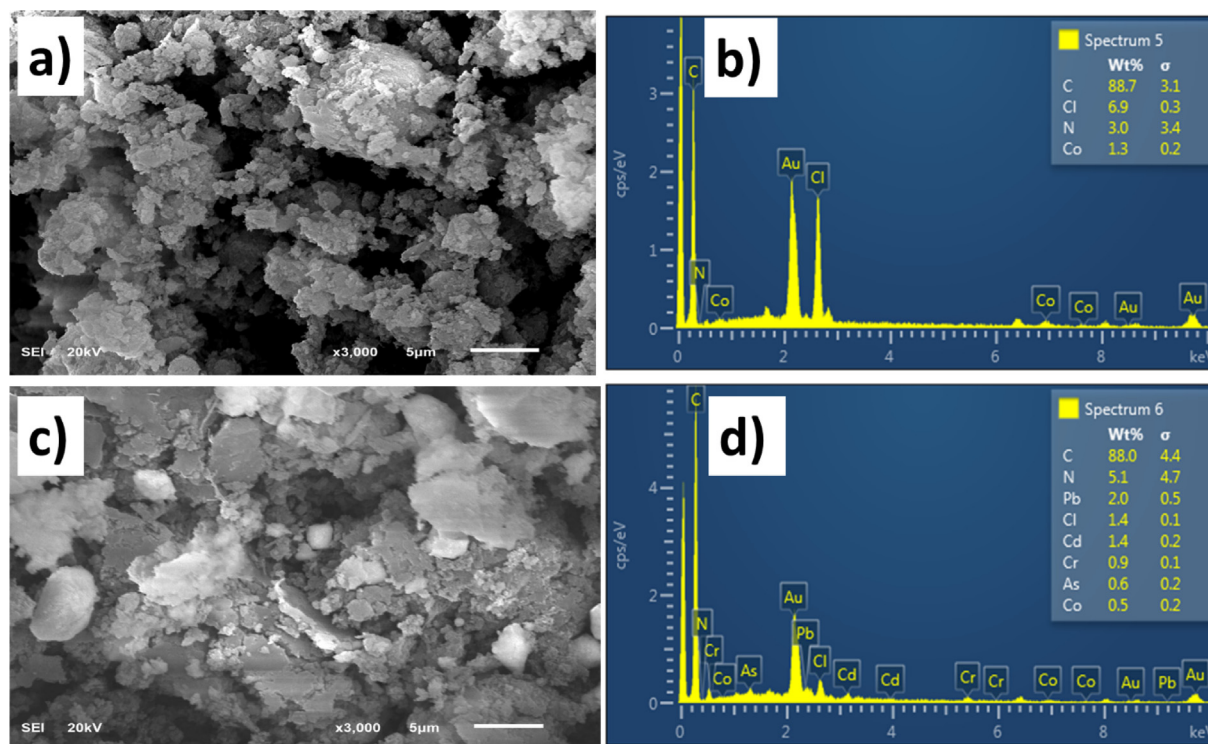


**Fig. 5** SEM micrograph of [2-AA]CoCl<sub>3</sub> MIL adsorbent a) before and c) after adsorption and EDX images b) before and d) after adsorption in 5  $\mu$ m magnification.

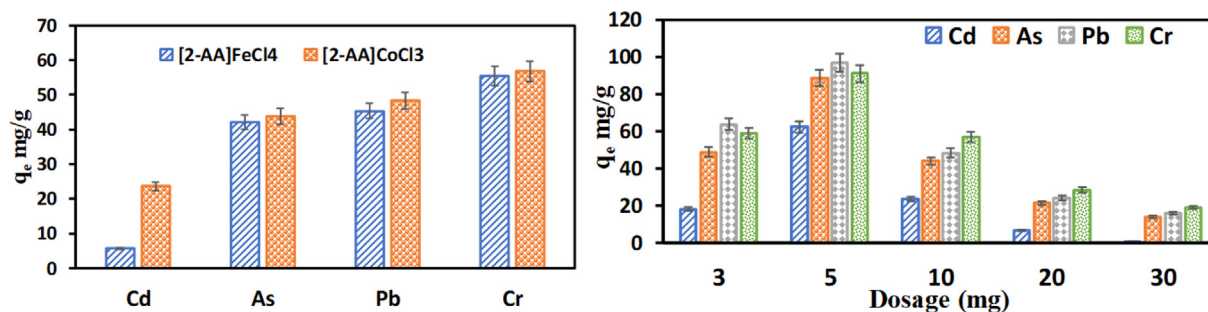


**Fig. 6** (a) Adsorption performance of MIL adsorbents and (b) Effect of [2-AA]CoCl<sub>3</sub> dosage.

iments. As shown in **Fig. SI-1**, the adsorption efficiency of [2-AA]CoCl<sub>3</sub> increases with increase in the pH, especially for Pb<sup>2+</sup> and Cr<sup>3+</sup>, which showed an excellent percent removal of more than 99% at pH 8 and 9 without major differences. However, by increasing the pH to beyond 9, it was observed that the metal ions precipitate and that is why higher pH was not considered. Therefore, pH 8 was chosen for the rest of the study. The pH result agrees with the isoelectric point of MIL, which shows a larger negative charge on the surface above pH 5, as shown in **Fig. 3(g)**, and this favors the electrostatic interaction between the cationic species and the large negative adsorption sites (Ali et al., 2018). In contrast, the lower pH below the net surface charge of zero exhibits positive active sites, which produce unfavorable electrostatic interaction that causes repulsion between the cationic metal ions

and the positively charged surface of MIL. Therefore, in general, the electrostatic interaction is the dominant factor affecting the adsorption behavior of the metal ions.

### 3.2.3. Effect of contact time on the adsorption efficiency of [2-AA]CoCl<sub>3</sub>

The contact time between the [2-AA]CoCl<sub>3</sub> MIL and metal ions in the solution affects the adsorption efficiency of the adsorbent. As presented in **Fig. SI-2**, the adsorption capacity increases from 5 min to 30 min, then stabilizes up to 60 min. It was however, noticed that the adsorption capacity decreases slightly after the 60 min contact time for some of the heavy metal ions. This behavior can be attributed to the saturation of the pores of the adsorbent (Changmai et al., 2018; Darama et al., 2021; Hastuti and Siswanta, 2015) or gradual

ionization leading to the formation of OH. Therefore, to save energy and time, 60 min was chosen as the equilibrium time for the subsequent adsorption studies.

### 3.2.4. Effect of metal ions concentration on the adsorption capacity of [2-AA]CoCl<sub>3</sub>

Generally, the metal ions concentration affects the adsorption capacity of adsorbents (see equation (1)). The effect of metal ions concentration was studied by varying the initial concentrations of the ions from 50 to 350 mg/L. The results show that the adsorption capacity of [2-AA]CoCl<sub>3</sub> increases with increase in concentration of metal ions up to 250 ppm (Fig. SI-3), then decreases slightly. This phenomenon may be due to the saturation of the active sites of the MIL. Based on the optimized result, the adsorption capacity of between 171 and 265 mg/g was recorded for the heavy metal ions.

### 3.2.5. Kinetics studies

The adsorption processes of the Cd<sup>2+</sup>, As<sup>3+</sup>, Pb<sup>2+</sup> and Cr<sup>3+</sup> heavy metal ions on the [2-AA]CoCl<sub>3</sub> adsorbent can be better understood using adsorption kinetic parameters. These parameters are typically derived from the pseudo-first order (LAGERGREIN, 1898) and pseudo-second order kinetic models (Ho and McKay, 1999) that are mathematically expressed by Lagergren rate equation (2) and Ho and McKay rate equation (3) respectively.

$$\ln(q_e - q_t) = \ln q_e - k_1 t \quad (2)$$

$$\frac{t}{q_t} = \frac{1}{k_2 q_e^2} + \frac{t}{q_e} \quad (3)$$

The  $q_t$  (mg/g) and  $q_e$  (mg/g) denote the amount of metal ions adsorbed at time  $t$  (min) and at equilibrium respectively. Similarly, the  $k_1$  (min<sup>-1</sup>) and  $k_2$  (g/mg·min) denote the pseudo-first order and pseudo-second order rate constants, respectively. If the adsorption processes for the heavy metal ions by [2-AA]CoCl<sub>3</sub> follows the pseudo-first order kinetic model, the plot of  $\ln(q_e - q_t)$  versus  $t$ (min) shown in Fig. SI-4(a) is expected to give a straight line with an intercept of  $\ln q_e$  and slope of  $-k_1$ . Similarly, if the adsorption processes proceeded via the pseudo-second order kinetics, then the plot of  $\frac{t}{q_t}$  versus  $t$ (min) presented in Fig. SI-4(b) is expected to give a straight line with an intercept of  $\frac{1}{k_2 q_e^2}$  and slope of  $\frac{1}{q_e}$ . Therefore, the obtained slopes and intercepts from the respective pseudo-first order and pseudo-second order plots are used to calculate the kinetic parameters  $k_1$ ,  $k_2$  and theoretical  $q_e(cal)$  that are summarized in Table 1. Consequently, the higher R<sup>2</sup> values for the pseudo-second order plots for all the heavy metal ions' adsorption on the [2-AA]CoCl<sub>3</sub> indicates that the

adsorption processes proceeded via the pseudo-second order pathway, thus the process is dominated by chemical interactions (Ho and McKay, 1999). Based on this, it may be inferred that the interaction between the heavy metal ions and [2-AA]CoCl<sub>3</sub> is electrostatic, between electron rich sites of the adsorbent and the metal ions. In addition, the closeness of experimental adsorption capacity ( $q_e(expt)$ ) with the pseudo-second order calculated adsorption capacity ( $q_e(cal)$ ) corroborate that the adsorption processes proceeded via the pseudo-second order pathway.

### 3.2.6. Adsorption isotherms

The adsorption isotherm studies is carried out to gain some insight into the nature of the interaction between the [2-AA]CoCl<sub>3</sub> adsorbent and the heavy metal ions. In this regard, the Langmuir and Freundlich isotherms models expressed by linear equations (4) and (5) respectively were used.

$$\frac{C_e}{q_e} = \frac{1}{K_L q_m} + \frac{C_e}{q_m} \quad (4)$$

$$\ln q_e = \ln K_F + \frac{1}{n} \ln C_e \quad (5)$$

$C_e$  ( $\frac{mg}{L}$ ) and  $q_e$  ( $\frac{mg}{g}$ ) denote the equilibrium concentration of adsorbate and adsorption capacity of the adsorbent, respectively.  $K_L$  and  $q_m$  denote Langmuir equilibrium constant and the maximum adsorption capacity of adsorbent respectively.  $K_F$  and  $n$  are Freundlich constants for a given adsorbate and adsorbent.

The Langmuir isotherm model is based on the assumption that the adsorption of the heavy metal ions occurs homogeneously on the surface of the [2-AA]CoCl<sub>3</sub> adsorbent using specific adsorption sites and energies. This model considered that steric hindrances and lateral interactions between adsorbate (heavy metal ions in this case) is not significant (Deng et al., 2009). Contrarily, the Freundlich isotherm model presumes that the adsorption of the heavy metal ions occurs heterogeneously, resulting to uneven distribution of adsorption energies over the [2-AA]CoCl<sub>3</sub> adsorption surfaces (Haghseresh and Lu, 1998). Therefore, by plotting  $\frac{C_e}{q_e}$  against  $C_e$  using equation (4), to get slope equal to  $\frac{1}{q_m}$  and intercept of  $\frac{1}{K_L q_m}$  (Fig. SI-5(a)), the  $K_L$  which relates directly with adsorption energy and  $q_m$  that signifies the monolayer adsorption capacity can both be determined. Similarly, the plot of  $\ln q_e$  against  $\ln C_e$  (using equation (5)) gives a slope equal to  $\frac{1}{n}$  and intercept of  $\ln K_F$  (Fig. SI-5(b)), and the constants  $n$  and  $K_F$  for the heavy metal ions' adsorption are determined accordingly (J. Zeldowitsch, 1934). The adsorption isotherm parameters are summarized in Table 2, and the correlation

**Table 1** Kinetic parameters for adsorption of heavy metal ions by [2-AA]CoCl<sub>3</sub> MIL.

Ion	$q_e(exp)$ (mg/g)	Pseudo-first order			Pseudo-second order		
		$k_1$ (min <sup>-1</sup> )	$q_e(cal)$ (mg/g)	R <sup>2</sup>	$k_2(10^4)$ (g/mg·min)	$q_e(cal)$ (mg/g)	R <sup>2</sup>
Cd	106.6	0.286	544	0.9352	6.84	142.8	0.9920
As	116.4	0.325	190	0.8682	20.6	131.6	0.9876
Pb	82.0	0.140	56.8	0.9634	28.8	91.7	0.9964
Cr	115.2	0.215	284	0.9142	9.35	140.8	0.9673

**Table 2** Isotherm parameters for adsorption of heavy metal ions on [2-AA]CoCl<sub>3</sub> MIL.

Langmuir isotherm				Freundlich isotherm		
Ion	$q_m$ (mg/g)	$K_L(10^3)$ (L/mg)	$R^2$	$n$	$K_F$	$R^2$
Cd	227.3	16.3	0.9789	2.22	16.6	0.9096
As	357.1	9.3	0.9705	1.94	14.7	0.8959
Pb	344.8	8.7	0.9875	2.05	15.8	0.9502
Cr	285.7	15.0	0.9677	2.20	18.1	0.8247

coefficient values ( $R^2$ ) of both models is used to evaluate the model that best fit the nature of the interaction between the [2-AA]CoCl<sub>3</sub> adsorbent and the heavy metal ions. Consequently, the  $R^2$  values of Langmuir adsorption isotherm nears one more than the  $R^2$  values of Freundlich adsorption isotherm, thus the heavy metal ions adsorption isotherm is best described by the Langmuir model which implies that the adsorption occurs homogeneously on the surface of the [2-AA]CoCl<sub>3</sub> adsorbent. In addition, Langmuir model has shown that the [2-AA]CoCl<sub>3</sub> adsorbent has demonstrated a remarkable performance in the removal of these heavy metal ions with maximum adsorption capacity ( $q_m$ ) in the range of 227 –

357 mg/g. The adsorption capacity of Cd<sup>2+</sup>, Pb<sup>2+</sup>, As<sup>3+</sup>, and Cr<sup>3+</sup> onto [2-AA]CoCl<sub>3</sub> adsorbent was compared with other adsorbents in recent published works (Table 3), and the [2-AA]CoCl<sub>3</sub> adsorbent performs quite well in the adsorption of Cd<sup>2+</sup>, Pb<sup>2+</sup>, As<sup>3+</sup>, and Cr<sup>3+</sup> compared to the adsorbents earlier reported.

### 3.2.7. Selectivity of [2-AA]CoCl<sub>3</sub> for Cd<sup>2+</sup>, Pb<sup>2+</sup>, As<sup>3+</sup>, and Cr<sup>3+</sup>

The selectivity of [2-AA]CoCl<sub>3</sub> for Cd<sup>2+</sup>, Pb<sup>2+</sup>, As<sup>3+</sup>, and Cr<sup>3+</sup> was studied by introducing 150 ppm each of Ca<sup>2+</sup>, K<sup>+</sup>, Na<sup>+</sup> and Mg<sup>2+</sup> as competitive ions in the sample solution containing 150 ppm each of Cd<sup>2+</sup>, Pb<sup>2+</sup>, As<sup>3+</sup>, and Cr<sup>3+</sup>. It was observed that even in the presence of other competitive metal ions, the [2-AA]CoCl<sub>3</sub> still exhibited superior adsorption performance for Cd<sup>2+</sup>, Pb<sup>2+</sup>, As<sup>3+</sup>, and Cr<sup>3+</sup> (Fig. SI-6), with adsorption capacity in the range of 206 – 286 mg/g. On the other hand, the adsorption capacity of Ca<sup>2+</sup>, K<sup>+</sup>, Na<sup>+</sup> and Mg<sup>2+</sup> is within the range of 20 – 34 mg/g (Table 4). The selectivity coefficient ( $K_{M/M'}$ ) of [2-AA]CoCl<sub>3</sub> for the targeted heavy metal ions (M) over other competitive metal ions (M') is calculated using the equation (6) (Ganiyu et al., 2016):

$$K_{M/M'} = \frac{K_d(M)}{K_d(M')} \quad (6)$$

Where  $K_d$  signifies the distribution coefficient of the metal ions and is calculated using equation (7):

$$K_d = \left( \frac{C_o - C_e}{C_e} \right) * \frac{V}{m} \quad (7)$$

Large value of  $K_d$  implies large adsorption of metal ion by adsorbent and vice-versa. Table 4 shows the  $K_d$  values of all the ions, and it is observed that the Cd<sup>2+</sup>, Pb<sup>2+</sup>, As<sup>3+</sup>, and Cr<sup>3+</sup> have larger  $K_d$  values, especially As<sup>3+</sup> ( $K_d = 460$  mL/g) than the Ca<sup>2+</sup>, K<sup>+</sup>, Na<sup>+</sup> and Mg<sup>2+</sup> ions. Similarly, the adsorption capacity of the targeted metal ions is in the range of 206–286 mg/g while the adsorption capacity of the interfering ions is 20–34 mg/g. In addition, the selectivity coefficient

**Table 3** Comparison of 2-anthracene ammonium trichlorocobaltate (II) adsorbent with other published work.

Adsorbent and method	Metal ion	Maximum adsorption capacities	Ref.
Mixture of magnetic graphite oxide and sand as a medium in a fixed-bed column	Cd	14.400 mg/g	(Ghasemabadi et al., 2018)
	Pb	49.856 mg/g	
	Cr	11.616 mg/g	
	As	8.976 mg/g	
Cassava root husk-derived biochar loaded with ZnO nanoparticles	Pb	3630.140 mg/g	(Tho et al., 2021)
	Cd	42.05 mg/g	
	As	39.52 mg/g	
	Cr	28.37 mg/g	
Shanghai silty clay (SSC)	Cd	8.90 mg/g	(Wang and Zhang, 2021)
	Pb	26.46 mg/g	
	Cr	1.85 mg/g	
	As	2.80 mg/g	
2-anthracene ammonium trichlorocobaltate (II) ([2-AA]CoCl <sub>3</sub> )	Cd	227.3 mg/g	This work
	Pb	344.8 mg/g	
	Cr	285.7 mg/g	
	As	357.1 mg/g	

**Table 4** Selective adsorption of targeted metal ions by [2-AA]CoCl<sub>3</sub>.

Metal ions	$C_o$ (ppm)	$C_e$ (ppm)	$q_e$ (mg/g)	$K_d$ (mL/g)	$K_{M/Mg}$	$K_{M/K}$	$K_{M/Na}$	$K_{M/Ca}$
Cd	138	35.0	206	5.88	22.8	22.5	34.8	39.4
As	143	0.62	285	460	1783	1760	2724	3080
Pb	147	4.65	284	61.2	237	234	362	410
Cr	141	3.57	275	77.0	299	295	456	516
Mg	145	129	33.2	0.26				
K	146	129	33.8	0.26				
Na	141	130	21.9	0.17				
Ca	145	135	20.1	0.15				

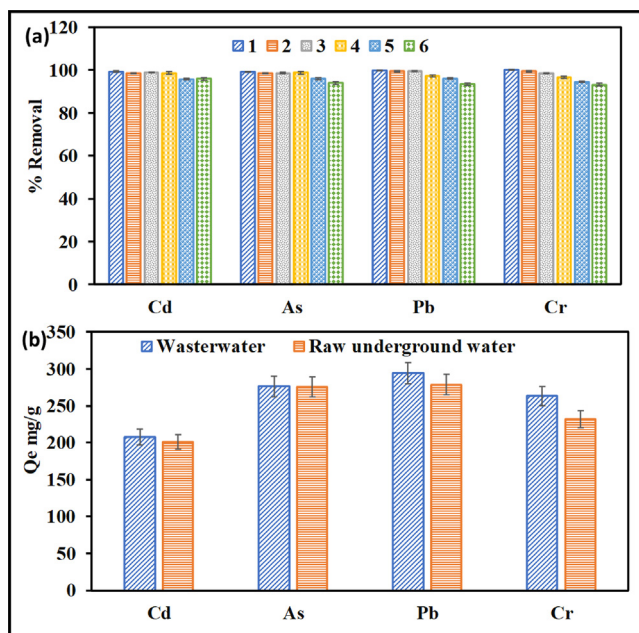


**Fig. 7** (a) Regeneration and reuse of MIL, [2-AA]CoCl<sub>3</sub> for 6 consecutive times for the adsorption of the metal ions Cd (II), As (II), Pb (II) and Cr(III) by using 1 M HNO<sub>3</sub>; (b) Adsorption performance of [2-AA]CoCl<sub>3</sub> MIL adsorbent using real raw underground and wastewater samples spiked with 150 ppm each of the targeted metal ions.

( $K_{M/M'}$ ) of each of the targeted metal ions is 2–3 orders of magnitude higher than those of the interfering metal ions. This further confirms the high selectivity of [2-AA]CoCl<sub>3</sub> for the targeted heavy metal ions.

### 3.2.8. Regeneration studies

Recycling of the adsorbent was studied to evaluate the loss of activity and possible reusability of the [2-AA]CoCl<sub>3</sub> MIL after it has been used for heavy metal ions' adsorption. Thus, after the adsorption, the adsorbent was recovered for reuse by centrifuging at 3500 rpm. Then washed thoroughly with 1 M nitric acid at pH 3 until no residue of the metal ions was detectable in the supernatant solution. Finally, the adsorbent was dried at 50 °C before reuse. It was discovered that the [2-AA]CoCl<sub>3</sub> MIL could be reused six times with excellent adsorption efficiency of more than 93% (Fig. 7(a)). Interestingly, similar results were obtained when real wastewater and ground water resources were spiked with 150 ppm each of the targeted metal ions as shown in Fig. 7(b). This shows the practicality of the [2-AA]CoCl<sub>3</sub> MIL adsorbent in the selective removal of Cd<sup>2+</sup>, Pb<sup>2+</sup>, As<sup>3+</sup>, and Cr<sup>3+</sup> metal ions in a complex matrices.

## 4. Conclusion

This study presents the adsorption potential of two novel 2-anthracene ammonium-based magnetic ionic liquids (MILs) in the removal of Cd<sup>2+</sup>, Pb<sup>2+</sup>, As<sup>3+</sup>, and Cr<sup>3+</sup> from ground and wastewater resources. The MILs, 2-anthracene ammonium tetrachloroferrate (III) or 2-anthracene ammonium trichlorocobaltate (II) ([2-AA]CoCl<sub>3</sub>), were synthesized by protonation of 2-aminoanthracene, followed by complexation with FeCl<sub>3</sub>/CoCl<sub>2</sub>. The [2-AA]CoCl<sub>3</sub> with slightly higher

adsorption capacity for removal of the targeted metal ions was used for optimization of adsorption parameters and kinetics and isotherms studies. The [2-AA]CoCl<sub>3</sub> performed efficiently in both neutral and alkaline solutions, and equilibrium adsorption was recorded within 60 min contact time. The adsorption process proceeded via the Pseudo-second order pathway and the Langmuir isotherm model fitted the adsorption process, with maximum adsorption capacity in the range of 227 – 357 mg/g. In addition, the [2-AA]CoCl<sub>3</sub> is selective to the targeted metal ions with large distribution coefficient and selectivity coefficient in the order of 2–3 against the interfering ions. The [2-AA]CoCl<sub>3</sub> has demonstrated practicality as adsorbent for the selective removal of the targeted metal ions with an adsorption efficiency of above 90% after 6 times reuse and with similar performance in real raw underground and wastewater samples.

The authors declare that they have no known competing financial interests that could have appeared to influence the work reported in this paper.

### CRedit authorship contribution statement

**Ahmed Abdi Hassan:** Conceptualization, Data curation, Formal analysis, Methodology, Writing – original draft. **Abdulka-dir Tanimu:** Investigation, Methodology, Visualization, Writing – original draft, Writing – review & editing. **Saheed A. Ganiyu:** Methodology, Writing – review & editing. **Ibrahim Y. Yaagoob:** Methodology, Data curation. **Khalid Alhooshani:** Investigation, Methodology, Visualization, Supervision, Writing – review & editing.

### Declaration of Competing Interest

The authors declare that they have no known competing financial interests or personal relationships that could have appeared to influence the work reported in this paper.

### Acknowledgement

The financial support provided by the King Fahd University of Petroleum and Minerals, through the project No. DSR SL191003 is acknowledged.

### Appendix A. Supplementary material

Supplementary data to this article can be found online at <https://doi.org/10.1016/j.arabjc.2022.104136>.

### References

- Abdi Hassan, A., Sajid, M., Al Ghafly, H., Alhooshani, K., 2020. Ionic liquid-based membrane-protected micro-solid-phase extraction of organochlorine pesticides in environmental water samples. *Microchem. J.* 158, 105295.
- Ali, J., Wang, H., Ifthikar, J., Khan, A., Wang, T., Zhan, K., Shahzad, A., Chen, Z., Chen, Z., 2018. Efficient, stable and selective adsorption of heavy metals by thio-functionalized layered double hydroxide in diverse types of water. *Chem. Eng. J.* 332, 387–397.
- Almeida, J.C., Cardoso, C.E.D., Tavares, D.S., Freitas, R., Trindade, T., Vale, C., Pereira, E., 2019. Chromium removal from contaminated waters using nanomaterials – a review. *TrAC, Trends Anal. Chem.* 118, 277–291.
- Ayangbenro, A.S., Babalola, O.O., 2017. A new strategy for heavy metal polluted environments: a review of microbial biosorbents. *Int. J. Environ. Res. Public Health* 14, 94.

- Azimi, A., Azari, A., Rezakazemi, M., Ansarpour, M., 2017. Removal of Heavy Metals from Industrial Wastewaters: a review. *Chem-BioEng. Rev.* 4, 37–59.
- Bolisetty, S., Peydayesh, M., Mezzenga, R., 2019. Sustainable technologies for water purification from heavy metals: review and analysis. *Chem. Soc. Rev.* 48, 463–487.
- Breite, D., Went, M., Thomas, I., Prager, A., Schulze, A., 2016. Particle adsorption on a polyether sulfone membrane: How electrostatic interactions dominate membrane fouling. *RSC Adv* 6, 65383–65391.
- Changmai, M., Banerjee, P., Nahar, K., Purkait, M.K., 2018. A novel adsorbent from carrot, tomato and polyethylene terephthalate waste as a potential adsorbent for Co (II) from aqueous solution: Kinetic and equilibrium studies. *J. Environ. Chem. Eng.* 6, 246–257.
- Darama, S.E., Gürkan, E.H., Terzi, Ö., Çoruh, S., 2021. Leaching performance and zinc ions removal from industrial slag leachate using natural and biochar walnut shell. *Environ. Manage.* 67, 498–505.
- de Souza, R.M., Seibert, D., Quesada, H.B., de Jesus Bassetti, F., Fagundes-Klen, M.R., Bergamasco, R., 2020. Occurrence, impacts and general aspects of pesticides in surface water: a review. *Process Saf. Environ. Prot.* 135, 22–37.
- Deng, H., Yang, L., Tao, G., Dai, J., 2009. Preparation and characterization of activated carbon from cotton stalk by microwave assisted chemical activation-application in methylene blue adsorption from aqueous solution. *J. Hazard. Mater.* 166, 1514–1521.
- Dinake, P., Kelebemang, R., Sehube, N., 2019. A comprehensive approach to speciation of lead and its contamination of firing range soils: a review. *Soil Sediment Contamin.: Int. J.* 28, 431–459.
- Erdem Yayayürük, A., Yayayürük, O., Tukenmez, E., Karagoz, B., 2021. Multidentate amine ligand decorated hairy brushes on PS-DVB microbeads for Cd (II) removal from water samples. *Sep. Sci. Technol.* 56, 2170–2182.
- Fiyadh, S.S., AlSaadi, M.A., Jaafar, W.Z., AlOmar, M.K., Fayaed, S. S., Mohd, N.S., Hin, L.S., El-Shafie, A., 2019. Review on heavy metal adsorption processes by carbon nanotubes. *J. Clean. Prod.* 230, 783–793.
- Fuerhacker, M., Haile, T.M., Kogelnig, D., Stojanovic, A., Keppler, B., 2012. Application of ionic liquids for the removal of heavy metals from wastewater and activated sludge. *Water Sci. Technol.* 65, 1765–1773.
- Ganiyu, S.A., Alhooshani, K., Sulaiman, K.O., Qamaruddin, M., Bakare, I.A., Tanimu, A., Saleh, T.A., 2016. Influence of aluminium impregnation on activated carbon for enhanced desulfurization of DBT at ambient temperature: Role of surface acidity and textural properties. *Chem. Eng. J.* 303, 489–500.
- Ghasemabadi, S.M., Baghdadi, M., Safari, E., Ghazban, F., 2018. Investigation of continuous adsorption of Pb (II), As (III), Cd (II), and Cr (VI) using a mixture of magnetic graphite oxide and sand as a medium in a fixed-bed column. *J. Environ. Chem. Eng.* 6, 4840–4849.
- Gokmen, F.O., Yaman, E., Temel, S., 2021. Eco-friendly polyacrylic acid based porous hydrogel for heavy metal ions adsorption: characterization, adsorption behavior, thermodynamic and reusability studies. *Microchem. J.* 168, 106357.
- Guo, Y., Qi, P.S., Liu, Y.Z., 2017. A review on advanced treatment of pharmaceutical wastewater, in: *IOP Conference Series: Earth and Environmental Science*. IOP Publishing, p. 12025.
- Haghseresht, F., Lu, G.Q., 1998. Adsorption characteristics of phenolic compounds onto coal-reject-derived adsorbents. *Energy Fuels* 12, 1100–1107.
- Hassan, M.M., Carr, C.M., 2018. A critical review on recent advancements of the removal of reactive dyes from dyehouse effluent by ion-exchange adsorbents. *Chemosphere* 209, 201–219.
- Hassan, A.A., Sajid, M., Tanimu, A., Abdulazeez, I., Alhooshani, K., 2020. Removal of methylene blue and rose bengal dyes from aqueous solutions using 1-naphthylammonium tetrachloroferrate (III). *J. Mol. Liq.* 114966
- Hassan, A.A., Tanimu, A., Alhooshani, K., 2021. Iron and cobalt-containing magnetic ionic liquids for dispersive micro-solid phase extraction coupled with HPLC-DAD for the preconcentration and quantification of carbamazepine drug in urine and environmental water samples. *J. Mol. Liq.* 336, 116370.
- Hastuti, B., Siswanta, D., 2015. Biosorption of Pb (II) ion by crosslinked pectin-CMC with BADGE (bisphenol A diglycidyl ether) through reflux method. *Int. J. Environ. Sci. Develop.* 6, 77–82.
- Hawkes, S.J., 1997. What is a “heavy metal”? *J. Chem. Educ.* 74, 1374.
- Ho, Y.S., Mckay, G., 1999. Pseudo-second order model for sorption processes 34, 451–465
- Hoslett, J., Massara, T.M., Malamis, S., Ahmad, D., van den Boogaert, I., Katsou, E., Ahmad, B., Ghazal, H., Simons, S., Wrobel, L., Jouhara, H., 2018. Surface water filtration using granular media and membranes: a review. *Sci. Total Environ.* 639, 1268–1282.
- Hu, B., Ma, Y., Wang, N., 2020. A novel water pollution monitoring and treatment agent: Ag doped carbon nanoparticles for sensing dichromate, morphological analysis of Cr and sterilization. *Microchem. J.* 157, 104855.
- Joo, S.H., Tansel, B., 2015. Novel technologies for reverse osmosis concentrate treatment: a review. *J. Environ. Manage.* 150, 322–335.
- Kakaei, S., Khameneh, E.S., Hosseini, M.H., Moharreri, M.M., 2020. A modified ionic liquid clay to remove heavy metals from water: investigating its catalytic activity. *Int. J. Environ. Sci. Technol.* 17, 2043–2058.
- Katheresan, V., Kansedo, J., Lau, S.Y., 2018. Efficiency of various recent wastewater dye removal methods: a review. *J. Environ. Chem. Eng.* 6, 4676–4697.
- Khulbe, K.C., Matsuura, T., 2018. Removal of heavy metals and pollutants by membrane adsorption techniques. *Appl. Water Sci.* 8, 1–30.
- Körpınar, B., Yayayürük, A.E., Yayayürük, O., Akat, H., 2021. Thiol-ended polycaprolactone: synthesis, preparation and use in Pb (II) and Cd (II) removal from water samples. *Mater. Today Commun.* 29, 102908.
- Korte, N.E., Fernando, Q., 1991. A review of arsenic (III) in groundwater. *Crit. Rev. Environ. Control* 21, 1–39.
- LAGERGREN, S.K., 1898. About the Theory of So-called Adsorption of Soluble Substances. *Sven. Vetenskapsakad. Handlingar* 24, 1–39.
- Lakherwal, D., 2014. Adsorption of heavy metals: a review. *Int. J. Environ. Res. Develop.* 4, 41–48.
- Maia, L.C., Soares, L.C., Alves Gurgel, L.V., 2021. A review on the use of lignocellulosic materials for arsenic adsorption. *J. Environ. Manage.* 288, 112397.
- Medeiros, A.M.M.S., Parize, A.L., Oliveira, V.M., Neto, B.A.D., Bakuzis, A.F., Sousa, M.H., Rossi, L.M., Rubim, J.C., 2012. Magnetic ionic liquids produced by the dispersion of magnetic nanoparticles in 1-n-butyl-3-methylimidazolium bis (trifluoromethanesulfonyl) imide (BMI. NTf<sub>2</sub>). *ACS Appl. Mater. Interfaces* 4, 5458–5465.
- Ojuederie, O.B., Babalola, O.O., 2017. Microbial and plant-assisted bioremediation of heavy metal polluted environments: a review. *Int. J. Environ. Res. Public Health* 14, 1504.
- Pendergast, M.M., Hoek, E.M.V., 2011. A review of water treatment membrane nanotechnologies. *Energy Environ. Sci.* 4, 1946–1971.
- Pratish, A., Kumar, A., Hu, Z., 2018. Adverse effect of heavy metals (As, Pb, Hg, and Cr) on health and their bioremediation strategies: a review. *Int. Microbiol.* 21, 97–106.
- Pyrzynska, K., 2019. Removal of cadmium from wastewaters with low-cost adsorbents. *J. Environ. Chem. Eng.* 7, 102795.
- Ramana, V.V., Sastry, K.S., 1994. Chromium toxicity in *Neurospora crassa*. *J. Inorg. Biochem.* 56, 87–95.

- Renge, V.C., Khedkar, S.V., Pande, S.V., 2012. Removal of heavy metals from wastewater using low cost adsorbents: a review. *Sci. Revs. Chem. Commun.* 2, 580–584.
- Sarkar, R., Pal, A., Rakshit, A., Saha, B., 2021. Properties and applications of amphoteric surfactant: A concise review. *J. Surfactants Deterg* 24, 709–730.
- Stojanovic, A., Keppler, B.K., 2012. Ionic liquids as extracting agents for heavy metals. *Sep. Sci. Technol.* 47, 189–203.
- Tanimu, A., Alhooshani, K., 2021. Insight into the syntheses, performances and mechanisms of organically modified adsorbents for mercury ion sensing and removal. *J. Environ. Chem. Eng.* 9, 105833.
- Tanimu, A., Muhammad Sajid Jillani, S., Ganiyu, S.A., Chowdhury, S., Alhooshani, K., 2021. Multivariate optimization of chlorinated hydrocarbons' micro-solid-phase extraction from wastewater using germania-decorated mesoporous alumina-silica sorbent and analysis by GC–MS. *Microchemical Journal* 160, 105674.
- Tho, P.T., Van, H.T., Nguyen, L.H., Hoang, T.K., Ha Tran, T.N., Nguyen, T.T., Hanh Nguyen, T.B., Nguyen, V.Q., Le Sy, H., Thai, V.N., Tran, Q.B., Sadeghzadeh, S.M., Asadpour, R., Thang, P.Q., 2021. Enhanced simultaneous adsorption of As(III), Cd(II), Pb(II) and Cr(VI) ions from aqueous solution using cassava root husk-derived biochar loaded with ZnO nanoparticles. *RSC Adv.* 11, 18881–18897.
- Vardhan, K.H., Kumar, P.S., Panda, R.C., 2019. A review on heavy metal pollution, toxicity and remedial measures: current trends and future perspectives. *J. Mol. Liq.* 290, 111197.
- Wang, T., Liu, W., Xiong, L., Xu, N., Ni, J., 2013. Influence of pH, ionic strength and humic acid on competitive adsorption of Pb(II), Cd(II) and Cr(III) onto titanate nanotubes. *Chem. Eng. J.* 215–216, 366–374.
- Wang, J., Zhang, W., 2021. Evaluating the adsorption of Shanghai silty clay to Cd(II), Pb(II), As(V), and Cr(VI): kinetic, equilibrium, and thermodynamic studies. *Environ. Monit. Assess.* 193, 131.
- Wieszcycka, K., Filipowiak, K., Wojciechowska, I., Aksamitowski, P., 2020. Novel ionic liquid-modified polymers for highly effective adsorption of heavy metals ions. *Sep. Purif. Technol.* 236, 116313.
- Xu, H., Zhu, S., Xia, M., Wang, F., 2021. Rapid and efficient removal of diclofenac sodium from aqueous solution via ternary core-shell CS@ PANI@ LDH composite: experimental and adsorption mechanism study. *J. Hazard. Mater.* 402, 123815.
- Yassin, F.A., El Kady, F.Y., Ahmed, H.S., Mohamed, L.K., Shaban, S.A., Elfadaly, A.K., 2015. Highly effective ionic liquids for biodiesel production from waste vegetable oils. *Egypt. J. Pet.* 24, 103–111.
- Yoo, J.-C., Lee, C., Lee, J.-S., Baek, K., 2017. Simultaneous application of chemical oxidation and extraction processes is effective at remediating soil Co-contaminated with petroleum and heavy metals. *J. Environ. Manage.* 186, 314–319.
- Zeldowitsch, J., 1934. Adsorption site energy distribution. *Acta Physicochim. U.R.S.S.* 1, 961–973.
- Zhu, S., Khan, M.A., Kameda, T., Xu, H., Wang, F., Xia, M., Yoshioka, T., 2022. New insights into the capture performance and mechanism of hazardous metals Cr<sup>3+</sup> and Cd<sup>2+</sup> onto an effective layered double hydroxide based material. *J. Hazard. Mater.* 426, 128062.